The Primary Self-Assembly Reaction of Bacteriophage λ *c*I Repressor Dimers Is to Octamer†

Donald F. Senear,*,‡ Thomas M. Laue,*,§ J. B. Alexander Ross,*,∥ Evan Waxman,∥ Steven Eaton,§ and Elena Rusinova∥

Department of Molecular Biology and Biochemistry, University of California, Irvine, California 92717, Department of Biochemistry, University of New Hampshire, Durham, New Hampshire 03824, and Department of Biochemistry, Mount Sinai School of Medicine, New York, New York 10029

Received January 22, 1993; Revised Manuscript Received March 23, 1993

ABSTRACT: Cooperative binding of the bacteriophage λ *c*I repressor dimer to specific sites of the phage operators O_R and O_L controls the developmental state of the phage. It has long been believed that cooperativity is mediated by self-assembly of repressor dimers to form tetramers which can then bind simultaneously to adjacent operator sites. As a first step in defining the individual energy contributions to binding cooperativity, sedimentation equilibrium and steady-state fluorescence anisotropy methods have been used to study the higher order assembly reactions of the free repressor in solution. Wild-type repressor with 5-hydroxytryptophan (5-OHTrp) substituted for the native tryptophan [Ross et al. (1992) *Proc. Natl. Acad. Sci. U.S.A. 89*, 12023–12027] and two mutant repressor proteins that bind cooperatively to O_R but have altered dimerization properties were also studied. We report here that the primary assembly mode of all four proteins is dimer to octamer. It is not dimer to tetramer as previously assumed. While tetramer does form as an assembly intermediate, dimer–octamer assembly is a concerted process so that tetramer is never a predominant species in solution. Sedimentation velocity experiments suggest that the octamer is highly asymmetric, consistent with an elongated shape. This conformation could allow octamers to bind simultaneously to all three operator sites at either O_R or O_L. Examination of tetramer and octamer concentrations suggests that both species could be involved in cooperative repressor–operator interactions. Our previous work used the unique spectral properties of 5-OHTrp to demonstrate that octamer binds single-operator DNA and is not dissociated to tetramer [Laue et al. (1993) *Biochemistry 32*, 2469–2472]. Taken together with the results presented here, octamers as well as tetramers must be considered in developing models to explain the cooperativity of λ *c*I repressor binding to operator DNA.

The right operator (O_R) of the bacteriophage λ is an important example of regulation of development, and has served as a paradigm for gene regulation at the level of initiation of transcription. The interactions of the phage-encoded *c*I and *cro* proteins with three operator sites at O_R constitute the primary control of the switch from lysogenic to lytic phage cycles [see Johnson, A. D., et al. (1981) for a review]. *c*I repressor dimers bind cooperatively to the three operator sites at O_R and also to three operator sites at the λ left operator, O_L. Cooperativity means that the affinity of a repressor dimer for any one site is enhanced when a dimer is already bound to an adjacent site. This cooperativity is crucial to the regulation of the developmental switch. It confers stability to the lysogenic phase, while also providing rapid and essentially irreversible induction of lysis in response to damage to the host cell chromosome (Johnson et al., 1979; Shea & Ackers, 1985). A long-standing goal of our studies of the λ repressor–O_R interactions has been to delineate the physical–chemical basis for this cooperativity.

It is generally believed that cooperative binding of the λ *c*I repressor to O_R involves self-association of repressor dimers to higher order oligomers, a process thought to be mediated by the C-terminal domain of the repressor. This interpretation is based on the demonstration of mass action assembly of free repressor dimers to higher order oligomers when the subunit concentration is in the micromolar range (Pirotta et al., 1970; Brack & Pirrotta, 1975). Such an assembly process would have sufficient free energy change to account for the observed cooperativity. A further correlation between cooperative binding and higher order assembly of free solution dimers is provided by isolated N-terminal repressor domains. These form dimers and also bind specifically to operator DNA, but do not assemble to higher order oligomers and do not bind cooperatively to O_R (Johnson et al., 1979). Though the higher order assembly of repressor dimers has never been examined in detail, it is widely believed that cooperativity in repressor–O_R interaction is strictly pairwise and that the explanation for this is that the predominant high-order oligomeric form of the repressor is tetramer (Ptashne, 1992).

Cooperative binding of the same, or of different, regulatory proteins to specific DNA sites is an important, general mechanism in the regulation of transcription initiation in both prokaryotes and eukaryotes. It is also important for other cellular processes such as recombination and replication. Protein–protein association to free oligomeric forms that provide multidentate ligands for DNA binding sites appears to be a common mechanism for cooperative binding of regulatory proteins to DNA [cf. Gralla (1989) for review]. The cooperativity produced by this mechanism includes thermodynamic contributions from several macromolecular interactions. First, the free energy change for protein–protein association always contributes favorably to cooperativity by providing oligomers that can interact simultaneously with

† Supported by Grants GM-41465 (D.F.S.) and GM-39750 (J.B.A.R.) from the National Institutes of Health and by Grant DIR9002027 (T.M.L.) from the National Science Foundation.

* Authors to whom correspondence should be addressed.
‡ University of California, Irvine.
§ University of New Hampshire.
∥ Mount Sinai School of Medicine.

0006-2960/93/0432-6179$04.00/0

multiple DNA sites. Second, binding of an oligomeric protein to multiple DNA sites might require structural rearrangement of the protein assembly, the DNA, or both. Such conformational changes contribute unfavorably to the cooperative interaction. An example of this is the free energy required to bend the DNA into loops when the protein binding sites are not close to one another on the DNA. The energetic consequences of loop formation have been considered in detail for the *Escherichia coli* Lac repressor, a bidentate tetramer (Mossing & Record, 1986; Bellomy et al., 1988; Brenowitz et al., 1991). Third, there can be thermodynamic linkage between protein–protein assembly and DNA binding. This means that the different oligomeric forms of the protein have different intrinsic DNA binding affinities. This will contribute favorably or unfavorably to cooperativity, depending on whether the higher order oligomers have greater or lower intrinsic affinity for operator sites. Fourth, the intrinsic operator DNA binding affinity of multidentate regulatory protein assembly can vary depending on how many of its binding sites are liganded by DNA. These allosteric interactions can be mediated by either the protein or the DNA, and can make either favorable or unfavorable contributions to cooperativity.

Our goal is to resolve the contributions of these processes to the energetics of cooperativity of λ *c*I repressor binding to operator DNA. One strategy to accomplish this would be to study the binding of single and of multiple operator DNA to the various oligomeric forms of the repressor, for example, by conducting binding studies as a function of repressor concentration over the range where repressor dimers self-associate to higher order oligomers. This is precluded, however, by the relatively high intrinsic affinity of the repressor dimer for operator DNA, compared to the affinity for self-association. It is evident that to understand cooperativity in repressor binding to DNA one must characterize opposing sides of a thermodynamic cycle. Therefore, our strategy is to compare the self-association of repressor dimers when free in solution to that when bound to DNA containing either single or multiple operator sites.

Here, we report on the self-association of free repressor. These studies constitute the first half of this strategy. A combination of analytical ultracentrifugation and steady-state fluorescence anisotropy was used to study the self-association of the wild-type repressor and of wild-type repressor for which native tryptophan has been substituted by 5-hydroxytryptophan (5-OHTrp) (Ross et al., 1992). The unique advantage of the modified repressor in this context is that 5-OHTrp provides a distinct spectral signal that permits examination of the self-association of repressor when bound to operator DNA. Such examination of the native Trp-containing repressor bound to DNA is precluded by spectral overlap between protein and DNA absorption (Laue et al., 1993). The operator binding and monomer–dimer self-association behavior of the 5-OHTrp analog is identical to that of wild-type repressor (Ross et al., 1992). Since our future objective is to study the interaction of higher order assemblies of λ repressor with DNA, we compare in this paper the higher order assembly of the 5-OHTrp-containing repressor with that of wild-type. We have also studied two mutant repressor proteins which bind cooperatively to O_R, but which have altered dimerization properties. The purpose of these studies is to examine any possible connection between monomer–dimer and dimer to higher order assembly. As we will show, all four proteins assemble in a single transition to form octamers, not tetramers, as the limiting species.

The free energy change per addition of dimer is less for dimer to tetramer association than for dimer to octamer association. This indicates that the dimer to octamer association reaction is a concerted process. Although tetramer does form as an assembly intermediate, it is never a predominant species. Throughout the physiological range of repressor concentrations in a λ lysogen, the concentrations of both octamers and tetramers are sufficient to saturate adjacent operator sites and thereby account for cooperativity. Further, our sedimentation velocity data suggest that the octamer is a highly asymmetric assembly, consistent with an elongated shape. Thus, octamer might bind simultaneously to all three operator sites at either O_R or O_L. If this is the case, octamer could be responsible for cooperativity when all three operators are liganded. Consequently, any model that involves higher order association of dimers to explain the cooperativity in repressor–operator DNA interactions must account for the free energy change for octamer formation.

MATERIALS AND METHODS

Repressor Preparation. Wild-type λ *c*I repressor protein was expressed in *E. coli* using the *tac*-promoted expression plasmid pEA300WT (Amnan et al., 1983) and purified as described (Brenowitz et al., 1986). Expression and purification of the 5-OHTrp-containing λ *c*I repressor protein were described recently (Ross et al., 1992). The full-length mutant repressors Ile-84→Ser (I84S) and Tyr-88→Cys (Y88C) were expressed in *E. coli* from the *tac*-promoted plasmids pMH236 and pTAC54-1, respectively. The expression plasmids were generous gifts from Robert Sauer (MIT). The mutant proteins were purified as described for the wild-type protein, with the exception that the I84S was loaded onto the AffiGel Blue column at 150 mM KCl instead of 100 mM KCl to prevent its precipitation at the lower salt concentration. All repressor preparations are conservatively judged to be greater then 95% pure on the basis of Coomassie-stained $NaDodSO_4$–polyacrylamide gels. Denaturing electrophoresis of the Y88C repressor under both reducing and nonreducing conditions confirmed that at least 95% exists in the form of disulfide cross-linked dimers.

Protein concentrations were estimated from the extinction coefficients at 230, 280, and 310 nm (whereas tryptophan, tyrosine, and 5-OHTrp absorb light at 280 nm, only 5-OHTrp has significant absorption at 310 nm). The 280-nm extinction coefficients of the proteins were calculated from the average 280-nm extinction coefficients for tryptophan (5500 M^{-1} cm^{-1}) and tyrosine (1200 M^{-1} cm^{-1}) residues in a protein (Wetlaufer, 1962) and the 280-nm extinction coefficient of 5-OHTrp incorporated in a polypeptide (4500 M^{-1} cm^{-1}; Ross et al., 1992) assuming additivity of absorbances. The 230- and 310-nm extinction coefficients were calculated from XL-A centrifuge absorption spectra (Laue et al., 1993) by comparing the absorbances at 230 nm and at 310 nm to that at 280 nm. To assess the linearity of the XL-A absorbances with respect to protein concentration, the A_{230}/A_{280} and A_{310}/A_{280} absorbance ratios were determined at different radial positions after sedimentation equilibrium had been attained at 10K and at 20K rpm. These ratios were constant provided the absorbances at the two wavelengths were between 0.01 and 1.60. When the absorbance at 230 nm exceeded 1.60, A_{230}/A_{280} changed monotonically, indicating deviation from Beer's law. When the absorbance at 310 nm was less than 0.01, A_{310}/A_{280} became uncertain, indicating imprecision in the absorbances less than 0.01.

Sedimentation Equilibrium Experiments. Proteins were prepared for centrifugation by exhaustive dialysis against 10

mM Tris, pH 8.0, 2.5 mM $MgCl_2$, 1.0 mM $CaCl_2$, 0.1 mM dithiothreitol, and either 50 mM (low salt) or 200 mM (high salt) KCl. High-speed sedimentation equilibrium experiments at high salt for the wild-type and 5-OHTrp repressors were conducted at 10K, 20K, 30K, and 40K rpm, 23 °C, in a Beckman XL-A analytical ultracentrifuge using an absorbance optical system, a 4-hole titanium rotor, 6-channel, 12-mm-thick charcoal-filled epon centerpieces, and fused silica windows. Repressor concentrations loaded were approximately 1.1, 0.35, and 0.11 mg/mL. Sedimentation data were acquired as an average of four absorbance measurements per radial position at a nominal radial spacing of 0.001 cm. Channels for which the maximum absorbance did not exceed 0.10 were excluded, because the signal to noise ratio was unacceptably low. The data sets used in the analysis were truncated to include only absorbance values less than 1.60, for which absorbance is linear with respect to protein concentration.

For all other combinations of repressors and conditions, sedimentation equilibrium experiments were conducted using short column cells (0.7 mm) (Yphantis, 1960) and Rayleigh interference optics in a Beckman Model E analytical ultracentrifuge equipped with electronic speed control, RTIC temperature controller (23.3 °C), and a pulsed laser diode light source (670 nm). Data were acquired at speeds of 10K, 20K, 30K and 40K rpm using a television camera based, on-line data acquisition and analysis system (Laue, 1981; Laue et al., 1992). Samples were loaded at concentrations of approximately 1.8, 0.9, 0.45, and 0.2 mg/mL for experiments at high salt, and at 0.9–0.1 mg/mL for experiments conducted at low salt. Data were collected at intervals after estimated time to equilibrium and tested for equilibrium by subtracting successive scans (Yphantis, 1964). The data within the optical window were selected using the program REEDIT (kindly provided by David Yphantis).

Data were analyzed to estimate the dimer molecular weight and equilibrium association constants using the program NONLIN (Johnson, M. L., et al., 1981). One or more channels of sedimentation equilibrium data obtained at different loading concentrations, radial positions, and angular velocities were fit by simultaneous nonlinear least-squares to specified assembly schemes according to

$$C = \Delta C_j + \sum_{i=0}^{m} \exp[\gamma(i)] \tag{1a}$$

$$\gamma(1) = \ln C_0 + \sigma(r^2/2 - r_0^2/2) \tag{1b}$$

$$\gamma(i \neq 1) = N\gamma(1) + \ln K_N \tag{1c}$$

where C is the repressor concentration (in absorbance or fringe displacement units) observed at radial position r, ΔC_j is a base-line offset for channel j, C_0 is the concentration of repressor dimer at the meniscus (r_0), and σ is the reduced molecular weight, given by $\sigma = M_r(1-\bar{v}\rho)\omega^2/2RT$ (Yphantis & Waugh, 1956) where $\bar{v}$ is the partial specific volume, ρ is the buffer density, ω is the radial velocity, and R and T are the gas constant and absolute temperature, respectively. Conversion between reduced and nonreduced molecular weights used calculated buffer densities, ρ = 1.04 and ρ = 1.01 for 200 and 50 mM KCl, respectively (Laue et al., 1992), and $\bar{v}$ = 0.736 mL/g calculated from the amino acid composition (Cohn & Edsall, 1943). K_N is the equilibrium association constant for the assembly of dimers to N-mers. Different assembly schemes were considered by varying the number of terms [$\gamma(i \neq 1)$] and the values of N, as described in the text. Nonideality was not considered.

Sedimentation Velocity Experiments. These were conducted on the Beckman XL-A instrument described above using absorption optics. Experiments were conducted at 60K rpm, 20 °C, using a 4-hole titanium rotor, 2-channel, charcoal-filled epon centerpieces, and fused silica windows. Data were acquired as one absorbance measurement (280 nm) per radial position at a radial spacing of 0.003 cm. Sedimentation velocity studies were conducted at 3.3, 1.5, 0.51, and 0.17 mg/mL repressor at both high- and low-salt conditions. An apparent sedimentation coefficient was determined from the movement of the midpoint of the boundary. Derivative sedimentation coefficient distributions [$g(s)$] were calculated according to Stafford (1992).

Fluorescence Experiments. The steady-state fluorescence anisotropy of repressor proteins was measured as a function of their concentration at 20 °C using an SLM 4800 fluorometer that we have modified for single photon counting. The anisotropy, $\langle r \rangle$, is expressed as

$$\langle r \rangle = \frac{I_v - I_h}{I_v + 2I_h} \tag{2}$$

where I_v and I_h are the intensities detected through vertical and horizontal polarizers, respectively, when vertically polarized light is used to excite the sample. Excitation with horizontally polarized light was used to correct instrument bias in detection of the emission [see Badea and Brand (1979)]. The fluorescence emission was monitored using a 10-nm band-pass filter with maximum transmission at 340 nm. Excitation was at 270 nm. At this wavelength, the fluorescence anisotropy of N-acetyltryptophanamide in glycerol at 20 °C was constant (0.1605 ± 0.0005) when the excitation band-pass was 8 nm or less. The anisotropy decreased slightly to 0.157 when the excitation band-pass was increased to 16 nm. Therefore, a maximum excitation band-pass of 8 nm was used for measuring the protein anisotropy. The fluorescence intensity decay of the proteins was measured as previously described (Ross et al., 1992).

RESULTS

Self-Association of Wild-Type Repressor. Figure 1 presents results from sedimentation equilibrium experiments conducted on both the wild-type and 5-OHTrp repressors at 200 mM KCl. Three initial protein concentrations were centrifuged to equilibrium at 10K and at 20K rpm. Each channel was scanned at both 230 nm and 280 nm to maximize the range of concentrations that fall within the limits of accurate absorbance between 0.1 and 1.6. The channels containing 5-OHTrp repressor were also scanned at 310 nm, a wavelength for which the absorbances of both wild-type repressor and DNA are negligible (Laue et al., 1993). The combined data cover a range of repressor concentrations from 0.3 to 100 μM in total repressor subunits. At the low end of this concentration range, the repressor is over 90% dimeric (M_r = 52 420) based on a dimer dissociation constant of 4 nM (Koblan & Ackers, 1991). The remainder is monomeric.

Each of the radial absorbance scans in Figure 1 was analyzed according to eq 1, formulated to include only $\gamma(1)$, to determine the best whole channel, reduced molecular weight average. For both the wild-type and the 5-OHTrp repressors, the results (Table I) demonstrate the assembly of repressor dimers to higher order species over this concentration range. The self-polymerization follows a single assembly transition of dimers to a limiting species with molecular weight of about 220 000.

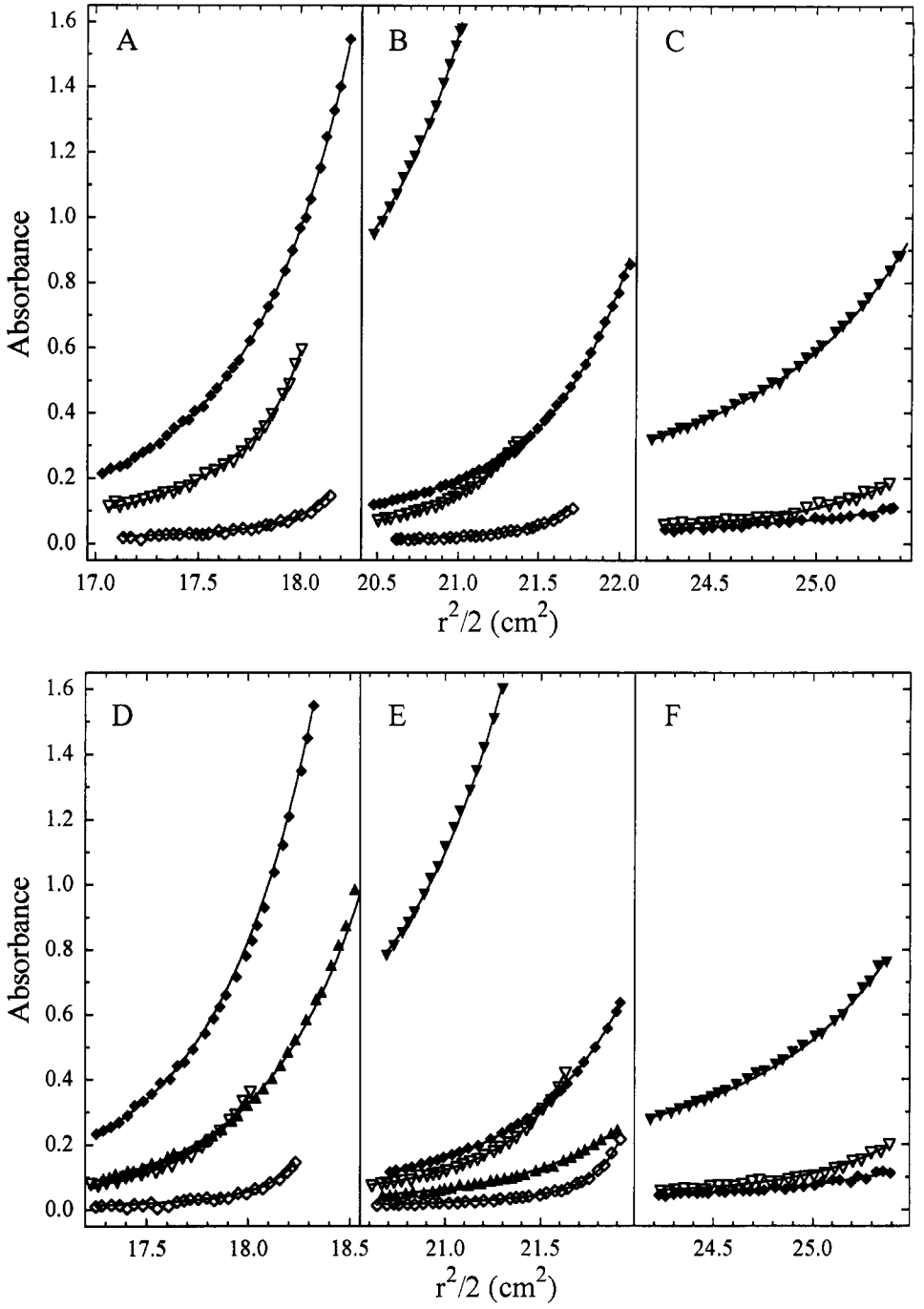

FIGURE 1: Sedimentation equilibrium data for wild-type and 5-OHTrp repressors, plotted as absorbance as a function of $r^2/2$. For clarity, only every fourth data point is shown. Experiments were conducted at 10 000 rpm (filled symbols) and at 20 000 rpm (open symbols) at 200 mM KCl and 23 °C. The three panels (A–C for wild-type; D–F for 5-OHTrp) represent data from channels with three different loading concentrations of 1.1, 0.35, and 0.11 mg/mL. Symbols represent absorbance scans at different wavelengths: (diamonds) 280 nm; (downward triangles) 230 nm; (upward triangles) 310 nm. The solid curves drawn through the points represent the best fit to the association of dimers to octamers, with the dimer molecular weight fixed at the value of 52 400 determined from the amino acid sequence. Parameter values are in Table III.

This is clearly inconsistent with the molecular weight of a repressor tetramer (105 000), but is instead consistent with the molecular weight of octamer (210 000).

The data in Figure 1 were more extensively analyzed by fitting to eq 1 where the number of terms and values of N were varied to account for different assembly schemes. Results of these analyses for the wild-type repressor are summarized in Table II. The best two-species fit, i.e., with σ, N and ln K_N (eq 1) all treated as adjustable parameters, yielded an assembly stoichiometry of 4.2 for an M_r = 57 700 species. The simplest interpretation is a dimer to octamer assembly scheme. Fixing N = 4 according to such a model yielded a dimer molecular weight, M_r = 51 520 ± 1110, which is within experimental uncertainty of the actual dimer molecular weight. The variance of the fit with N = 4 is actually slightly improved over the best two-species fit, indicating that treating N as an adjustable parameter is not justified.

Both the best two-species fit (Table II) and the single-channel molecular weight averages (Table I) could indicate assembly to species larger then octamer. Therefore, attempts were made to include either decamer or dodecamer as the limiting species in fitting the data in Figure 1. These data were also analyzed to include tetramers and hexamers as intermediates. Attempts to include the monomer–dimer

Table I: Concentration Dependence of Apparent Molecular Weight Averages for Wild-Type and 5-OHTrp λ cI Repressors at 200 mM KCl

sample	speed (rpm)	wavelength (nm)	[protein] (μM)[a]	σ (cm^{-2})[b]	M_r[c]	s (ODU)[d]
wild-type	10 000	280	20 (7.2, 54)	2.16 ± 0.05	201 600 ± 4 200	0.009
	10 000	280	11 (4.0, 29)	1.86 ± 0.03	178 800 ± 2 900	0.004
	10 000	230	5.1 (3.9, 6.6)	1.26 ± 0.08	120 900 ± 7 500	0.004
	10 000	280	2.4 (1.5, 3.8)	1.31 ± 0.27	126 000 ± 26 300	0.004
	10 000	230	2.2 (1.3, 3.7)	1.45 ± 0.07	139 400 ± 6 700	0.004
	20 000	280	1.9 (0.70, 5.0)	3.71 ± 0.46	88 800 ± 11 100	0.004
	20 000	280	1.4 (0.50, 3.7)	3.41 ± 0.20	81 600 ± 4 800	0.004
	20 000	230	1.1 (0.48, 2.5)	3.27 ± 0.17	78 200 ± 4 000	0.004
	20 000	230	0.62 (0.30, 1.3)	2.49 ± 0.07	59 900 ± 1 700	0.004
	20 000	230	0.43 (0.28, 0.77)	2.36 ± 0.30	56 500 ± 7 300	0.004
5-OHTrp	10 000	310	29 (8.6, 96)	2.31 ± 0.05	222 200 ± 5 100	0.006
	10 000	280	22 (7.9, 61)	2.26 ± 0.06	217 900 ± 5 600	0.009
	10 000	310	10 (4.2, 24)	1.99 ± 0.09	191 600 ± 8 400	0.002
	10 000	280	9.0 (3.9, 21)	2.01 ± 0.04	193 500 ± 3 900	0.003
	10 000	230	5.8 (3.8, 8.9)	1.36 ± 0.07	130 800 ± 6 400	0.006
	10 000	280	2.4 (1.5, 3.8)	1.46 ± 0.29	140 600 ± 27 600	0.005
	10 000	230	2.2 (1.3, 3.7)	1.36 ± 0.07	130 800 ± 6 700	0.005
	20 000	280	2.0 (0.54, 7.3)	4.89 ± 0.26	117 700 ± 6 300	0.004
	20 000	280	1.5 (0.44, 4.9)	5.13 ± 0.67	123 500 ± 16 100	0.006
	20 000	230	0.88 (0.37, 2.1)	2.84 ± 0.13	68 400 ± 3 100	0.004
	20 000	230	0.85 (0.40, 1.8)	3.41 ± 0.22	82 100 ± 5 300	0.005
	20 000	230	0.53 (0.29, 0.99)	2.29 ± 0.24	55 100 ± 5 800	0.004

[a] Approximate midchannel protein concentration. Meniscus and base concentrations are respectively indicated in parentheses. [b] Reduced molecular weight as defined by Yphantis and Waugh (1956) with 65% confidence interval (Johnson, M. L., et al., 1981). [c] Molecular weight (with 65% confidence interval) calculated from σ assuming $\bar{v}$ = 0.736 for the repressor and a solution density ρ = 1.040. [d] Square root of the variance of the fit.

Table II: Apparent Dimer Molecular Weights and Association Free Energy Changes for Assembly of Wild-Type λ cI Repressor at 200 mM KCl from Fits to Different Association Schemes[a]

	R_2–R_{2N}	R_2–R_8	R_2–R_4–R_8	R_2–R_4–R_8–R_{12}
dimer mol wt	57710 ± 96	51520 ■ 1110	53740 ± 830	45310 ± 860
N[b]	4.20 ± 0.01	4[e]	2, 4[e]	2, 4, 6[e]
ΔG_N[c]	−25.1 ± 0.1			
ΔG_4[c]			−7.0 ± 0.1	−7.1 ± 0.1
ΔG_8[c]		−22.9 ± 0.2	−23.0 ■ 0.1	−23.3 ± 0.1
ΔG_{12}[c]				−37.9 ± 0.2
s (ODU)[d]	0.0053	0.0052	0.0051	0.0050

[a] Data in Figure 1 were analyzed according to eq 1. Species included in each association scheme are related by the stoichiometries denoted by the values of N, listed in the second row. The fitted molecular weight of the smallest species is listed in the first row. This was interpreted to be dimer in each case, based on the correspondence between the fitted and actual dimer molecular weights. Thus, R_i in the column headings denote the species considered in each assembly scheme, where i is the stoichiometry of repressor subunits. R_2, R_4, and R_8 refer to dimers, tetramers, and octamers, respectively. R_{2N} in column 2 denotes that the stoichiometry of the higher order polymer was a fitted parameter. This column gives the best fit to a two-state assembly model. The confidence limits were nearly symmetrical for all fitted parameters, and so are presented as single ± values. These constitute estimates of the precision of the fitted parameters and do not necessarily reflect the accuracy of the values. [b] Assembly stoichiometry for the reaction: $N \cdot R_2 \rightleftharpoons R_{2N}$. [c] Free energy change for association of repressor dimers to higher order polymer whose stoichiometry, in subunits, is denoted by the value of the subscript. Values are in kilocalories per mole relative to a 1 M standard state. [d] Square root of the variance of the fit in absorbance units. [e] Parameters in list held fixed during fitting procedure.

equilibrium in the analysis failed. At the lowest repressor concentration, there is still insufficient monomer to characterize this transition. The only schemes that yielded satisfactory fits are shown in Table II. All of these include octamer. The scheme shown in the last column of Table II represents the assembly of dimers to tetramers, followed by the beginning of an isodesmic association of tetramers. An isodesmic association of dimers (i.e., $R_2 \leftrightarrow R_4 \leftrightarrow R_6 \leftrightarrow R_8 \leftrightarrow R_{10}$) resulted in a series of local minima in the variance, none of which constituted a satisfactory fit to the data. Each of these local minima had one or both ln K's (eq 1) equal to zero for formation of tetramer and hexamer, suggesting that there is at most only one intermediate between dimer and octamer.

Inclusion of tetramers or both tetramers and dodecamers to the dimer–octamer assembly scheme failed to yield a statistically meaningful improvement in either the variance (Table II) or the residual plots for the individual channels (not shown). In addition, the assembly free energy change for octamer formation was not significantly affected by inclusion of tetramer in the assembly scheme, and the assembly free energy changes for tetramer and for octamer were not affected by inclusion of dodecamer. The fits for which results are shown in Table II treated the dimer molecular weight as an adjustable parameter. In all cases, when the reduced molecular weight, σ, was fixed to correspond to the actual dimer molecular weight, there was no significant change either in the variance or in any of the fitted parameters.

The correspondence between the data and the dimer–octamer and dimer–tetramer–octamer assembly schemes was further examined by analyzing separately the 230- and 280-nm data for the wild-type and 5-OHTrp repressors. The concentration of dodecamer is small enough that it was neglected. These analyses exploit the very different (though overlapping) concentration ranges provided by scans at the two wavelengths (see Table I). The question we ask is whether the data provide an internally consistent description of the assembly transition when analyzed according to either model, as indicated by obtaining similar parameter values for the 230- and 280-nm data. In these analyses, σ either was a fitted parameter or was fixed to correspond to the actual dimer molecular weight. The results of these analyses (Table III) indicate the following three points. First, the 230- and 280-nm data for both the wild-type and 5-OHTrp repressors are consistent with a simple dimer–octamer assembly, and yield similar estimates of the assembly free energy change. The apparent dimer molecular weights differ for the 230- and 280-nm data (see Table III). These differences probably reflect the fact that the different wavelength data are for two different concentration ranges and hence the analysis results are affected differently by the presence of small amounts of low molecular weight contaminants. Nevertheless, both the 230- and the 280-nm data are well fit by an $R_2 \leftrightarrow R_8$ assembly scheme, and when all the data for either the wild-type or the 5-OHTrp repressor are considered together, the best estimate

Table III: Apparent Dimer Molecular Weights and Association Free Energy Changes for Repressor Assembly at 200 mM KCl Obtained from Separate Analysis of 230- and 280-nm Data for Wild-Type and 5-OHTrp Repressors[a]

repressor	λ (nm)	M_2[b]	ΔG_8[c]	s (ODU)[d]	M_2[b]	ΔG_4[c]	ΔG_8[c]	s (ODU)
wild-type	280	54 390 ± 860	−21.7 ± 0.3	0.0048	62 030 ± 5 780	−7.3 ± 0.4	−22.3 ± 0.2	0.004
		52 400[e]	−22.2 ± 0.3	0.0049	52 400[e]	+4.9 ± ∞	−22.2 ± 0.1	0.005
	230	45 810 ± 2 590	−23.1 ± 0.2	0.0051	46 460 ± 580	−6.0	−23.4 ± 0.1	0.005
		52 400[e]	−23.0 ± 0.2	0.0053	52 400[e]	−6.5 ± 0.2	−23.1 ± 0.1	0.005
	all	51 520 ± 1 100	−22.9 ± 0.2	0.0052	53 740 ± 830	−7.0 ± 0.1	−23.0 ± 0.1	0.005
		52 400[e]	−22.8 ± 0.2	0.0053	52 400[e]	−6.7 ± 0.2	−23.0 ± 0.1	0.005
5-OHTrp	280	39 040 ± 2 050	−23.0 ± 0.3	0.0046	39 910 ± 1 160	−6.4 ± 0.4	−23.2 ± 0.1	0.004
		52 400[e]	−22.7 ± 0.3	0.0055	52 400[e]	−7.3 ± ∞	−22.9 ± 0.1	0.005
	230	56 950 ± 1 390	−22.6 ± 0.2	0.0052	69 970 ± 1 830	−8.0 ± 0.4	−23.1 ± 0.4	0.004
		52 400[e]	−23.2 ± 0.2	0.0061	52 400[e]	±∞[f]	−23.2 ± 0.4	0.006
	all	56 980 ± 1 330	−22.5 ± 0.2	0.0054	63 080 ± 1 020	−7.1 ± 0.3	−22.7 ± 0.2	0.005
		52 400[e]	−22.9 ± 0.2	0.0061	52 400[e]	≥−6.1[g]	−23.0 ± 0.3	0.006

[a] Data in Figure 1 were analyzed according to dimer–octamer and dimer–tetramer–octamer assembly schemes using eq 1. The 280- and 230-nm data were separately analyzed, and then combined. For the 5-OHTrp repressor, the 310-nm data were also included in the analysis of all data. [b] Dimer molecular weight (with 65% confidence intervals) calculated from σ, as described for Table I. [c] Free energy changes in kilocalories per mole relative to a 1 M standard state for assembly of dimers to tetramers (ΔG_4) and octamers (ΔG_8). Values shown as ± or in parentheses are 65% confidence limits. [d] Square root of the variance of the fits in absorbance units. [e] Parameter held fixed during fitting procedure. [f] Convergence was not possible in this case. The ±∞ are confidence limits obtained from a grid search. [g] Convergence was not possible in this case. The value −6.1 kcal/mol is a limiting value found obtained from a grid search.

Table IV: Association Free Energy Changes for Wild-Type and Mutant Repressors at High- and Low-Salt Conditions[a]

	200 mM KCl			50 mM KCl		
repressor	ΔG_4	ΔG_8	s[b]	ΔG_4	ΔG_8	s[b]
wild-type		−22.8 ± 0.2	0.0053		−23.0 ± 0.2	0.015
	−6.7 ± 0.2	−23.0 ± 0.1	0.0051	−7.0 ± 0.3	−23.6 ± 0.2	0.015
5-OHTrp		−22.9 ± 0.2	0.0061		−23.1 ± 0.3	0.020
	≥−6.1	−23.0 ± 0.3	0.0061	−8.4 ± 0.3	−25.3 ± 0.5	0.019
I84S[c]		−19.5 ± 0.1	0.021		−23.0 ± 0.2	0.016
	−6.4 ± 0.1	−20.4 ± 0.1	0.021	−9.4 ± 0.3	−26.7 ± 0.6	0.014
Y88C		−22.9 ± 0.2	0.012		−21.0 ± 0.2	0.029
	−6.9 ± 0.2	−23.4 ± 0.2	0.012	−7.3 ± 0.2	−22.6 ± 0.2	0.025

[a] Free energy changes in kilocalories per mole relative to a 1 M standard state for assembly of dimers to tetramers (ΔG_4) and to octamers (ΔG_8) with 65% confidence limits. Data were analyzed assuming a repressor dimer molecular weight of 52 400. [b] Square root of the variance of the fits. These are in fringes displacement units except for the high-salt wild-type and 5-OHTrp fits, which are in absorbance units. [c] The low-salt I84S data were analyzed according to $R \leftrightarrow R_2 \leftrightarrow R_8$ and $R \leftrightarrow R_2 \leftrightarrow R_4 \leftrightarrow R_8$ assembly schemes, where the free energy for dimer formation, ΔG_2, was set equal to −7.5 kcal/mol based on analysis of the anisotropy data in Figure 2, as described in the text.

of dimer molecular weight is close to the actual value. Second, ΔG_4 for assembly of dimers to tetramers is not precisely resolved; the best estimate of its value is in the range −6 to −7 kcal/mol, and −7 kcal/mol is the lower limit. Third, ΔG_8 for assembly of dimers to octamers is about −23 kcal/mol; its estimation is unaffected by inclusion of tetramers in the model.

Effect of KCl on Self-Association of Wild-Type Repressor. Sedimentation equilibrium studies of the wild-type and 5-OHTrp repressors also were conducted at 50 mM KCl to assess the generality of the observation that the predominant assembly reaction is of dimer to octamer. The salt concentration was varied on the basis of the observations of Koblan and Ackers (1991), who demonstrated a substantial KCl concentration dependence to the monomer–dimer assembly reaction of the λ repressor, and of Senear and Batey (1991), who demonstrated a significant KCl concentration dependence to the cooperativity in repressor binding to O_R. Koblan and Ackers (1991) also showed that changes in other solution variables had negligible effects on monomer–dimer assembly. The KCl affect accounts for about a 10-fold increase in dimer stability at 200 mM KCl as compared to 50 mM KCl.

Experiments were conducted using the short column method (Yphantis, 1960) and interference optics. The radial concentration distributions observed by using short columns and interference optics were nearly identical to those observed using long columns and absorption optics. Analysis of the low salt (50 mM KCl) data produced results similar to those for the high-salt (200 mM KCl) data. When analyzed according to a dimer–octamer assembly model, the wild-type and 5-OHTrp repressor data yielded dimer M_r = 52 500 ± 1090 and 50 010 ± 1130, respectively. Both values are very near the expected dimer molecular weight of 52 400. When these data were analyzed according to an $R_2 \leftrightarrow R_4 \leftrightarrow R_8$ assembly scheme, the dimer molecular weight estimates deviated further from 52 400. The same result was obtained in the analysis of the high-salt data (Table III). This deviation reflects the general difficulty in obtaining precise parameter estimates for assembly schemes that include *small* fractions of assembly intermediates; the deviation is not a reflection of an incorrect model. For both repressors and both assembly schemes, the variance was not significantly altered when σ was fixed to correspond to an M_r 52 400 dimer.

Parameters for low- and high-salt assembly reactions are compared in Table IV. Comparing the estimates for ΔG_8 from the fits to the $R_2 \leftrightarrow R_8$ assembly scheme for the two salt concentrations, it is evident that nearly identical transitions are observed. Thus, the effect of KCl concentration on higher order oligomerization is negligible, in contrast to its affect on monomer–dimer assembly. More significantly, a comparison of the fits of the $R_2 \leftrightarrow R_4 \leftrightarrow R_8$ assembly scheme to the wild-type data at high and low salt indicates similar values for both ΔG_4 and ΔG_8. This confirms the conclusions drawn from the high-salt data that (1) tetramer is an intermediate in the assembly pathway and (2) tetramer is never a predominant species. It suggests that these are general results. Comparison of the fits of the $R_2 \leftrightarrow R_4 \leftrightarrow R_8$ assembly scheme

to the 5-OHTrp repressor data at high and low salt indicates statistically significant differences in both ΔG_4 and ΔG_8. Resolution of these free energies is less certain than indicated by the confidence limits. It is evident in the comparison of the variances of the fits for the $R_2 \leftrightarrow R_8$ and $R_2 \leftrightarrow R_4 \leftrightarrow R_8$ models that ΔG_4 and ΔG_8 are highly correlated. Thus, the apparent differences among ΔG_4 and among ΔG_8 values are artifacts due to this correlation [see Johnson and Frasier (1985)].

Self-Association of Mutant Repressors. Sedimentation equilibrium studies were also conducted on two mutant repressor proteins with altered dimerization properties to investigate the possibility of a connection between the monomer–dimer assembly reaction and the assembly of dimers to higher order polymers. Experiments were conducted at both low and high salt concentrations. The Y88C mutant spontaneously forms dimers that are covalently cross-linked by a cystine disulfide (Sauer et al., 1986). The I84S mutant has been suggested to form less stable dimers as compared to the wild-type (Hecht et al., 1983). Footprint titration analysis of the interaction of these mutants with λ O_R (Y. T. Huang and D. F. Senear, unpublished observations) indicates that both mutant repressors bind to the operator sites cooperatively, with high specificity, and with the usual order of affinity, $O_R1 > O_R2 > O_R3$.

Sedimentation equilibrium data for the I84S repressor at high salt, and for the Y88C repressor at both high and low salt, were analyzed as described above for wild-type repressor. Parameter values for Y88C (Table IV) are in line with those for the wild-type repressor, indicating that in this case there is no connection between monomer–dimer and dimer to higher order assembly. While the I84S higher order oligomers are significantly less stable at high salt than those of the other repressors, all show similar stability at low salt (see below). Thus, dimer to higher order assembly of I84S is KCl concentration dependent, though the direction of the effect is opposite to that observed by Koblan and Ackers (1991) for the monomer–dimer equilibrium. Evidently, quite different mechanisms are involved.

Fluorescence Anisotropy of I84S Self-Association at Low Salt. The expectation that I84S repressor is a weakly dimerizing mutant (Hecht et al., 1983), combined with the KCl concentration dependence of the wild-type repressor monomer–dimer equilibrium (Koblan & Ackers, 1991), presents a potential complication in the interpretation of sedimentation equilibrium data for I84S at low salt. Substantial overlap of the monomer–dimer and dimer to higher order assembly transitions would preclude accurate estimation of ΔG_4 and ΔG_8 because the range of sensitivity of the ultracentrifuge does not provide for characterization of the monomer–dimer equilibrium. Therefore, steady-state fluorescence anisotropy was used to monitor the monomer to dimer assembly of the I84S repressor at low salt, where the dimers are expected to be least stable. We previously used this technique to compare the monomer–dimer assembly reactions of the wild-type repressor and its 5-OHTrp analog under these experimental conditions (Ross et al., 1992). This yielded an equilibrium constant of 3×10^7 M^{-1}, which is within experimental error of the value 2.4×10^7 M^{-1}, obtained by Koblan and Ackers (1991) using a gel permeation chromatographic method. Anisotropy data for the I84S repressor over the concentration range 100 μM–40 nM are presented in Figure 2. The data reflect assembly of monomeric repressor to dimer with a transition midpoint occurring in the micromolar concentration range, indicating a substantially weaker association than for wild-type as anticipated by Hecht et al. (1983).

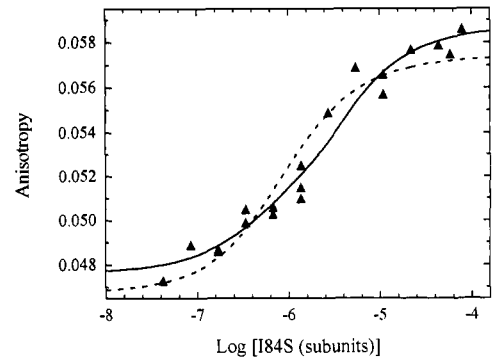

FIGURE 2: Steady-state fluorescence anisotropy of I84S repressor at 50 mM KCl. Curves drawn through the points for the I84S repressor show the fits according to $R \leftrightarrow R_4 \leftrightarrow R_8$ (solid curve) and $R \leftrightarrow R_2 \leftrightarrow R_4 \leftrightarrow R_8$ (dashed curve) assembly schemes. The square roots of the variances for these fits are 0.00077. The standard state is 1 M.

The fluorescence anisotropy demonstrates overlap between monomer–dimer and dimer to higher order assembly transitions (compare Figures 2 and 4, below). The analysis of these data must account for both dimers and higher order oligomers. The fluorescence intensity of the protein samples was directly proportional to the total protein concentration over the range where dissociation to monomers occurs. This allows both dimers and higher order assemblies to be accounted for by

$$\langle r \rangle_{obsd} = \langle r \rangle_o(R) + \langle r \rangle_f(2R_2 + 4R_4 + 8R_8) \qquad (3)$$

where $\langle r \rangle_{obsd}$, $\langle r \rangle_o$, and $\langle r \rangle_f$ are the observed, initial, and final anisotropies, respectively, and the R_i values are the concentrations of the polymeric forms of the repressor. Equation 3 assumes that the only steady-state anisotropy change occurs upon dimerization, with no further change upon dimer to higher order oligomer assembly. This assumption was confirmed experimentally by conducting separate experiments on the wild-type repressor. At 50 mM KCl, the dimer dissociation constant for the wild-type is 30 nM (Koblan & Ackers, 1991; Ross et al., 1992), so that the transition to dimer is essentially complete by 1 μM. The steady-state anisotropy of the wild-type repressor is constant over the range 0.6–4 μM (data not shown). According to the centrifuge results, 50% of wild-type repressor subunits are in tetrameric or octameric forms at 4 μM (see Figure 4, below).

To obtain parameter estimates consistent with both the sedimentation equilibrium and anisotropy data, the anisotropy data were first analyzed according to a simple monomer–dimer scheme, i.e., eq 3 with tetramer and octamer terms set equal to zero. Second, the sedimentation equilibrium data were analyzed according to $R \leftrightarrow R_2 \leftrightarrow R_8$ and $R \leftrightarrow R_2 \leftrightarrow R_4 \leftrightarrow R_8$ assembly schemes, with the monomer–dimer assembly association constant taken from the anisotropy data and treated as invariant. Third, the anisotropy data were analyzed by eq 3, with the association equilibrium constants for tetramers and octamers fixed. Only one round of this iterative analysis was required for the fits to converge and to provide precise estimates of all parameters. The results are reflected in the curves drawn through the anisotropy data in Figure 2.

Using a value from Table IV of $\Delta G_8 = -23.0$ kcal/mol, the anisotropy data are nicely described by the $R \leftrightarrow R_2 \leftrightarrow R_8$ assembly scheme and yield $\Delta G_2 = -7.5$ kcal/mol. The data are not well described by the $R \leftrightarrow R_2 \leftrightarrow R_4 \leftrightarrow R_8$ assembly scheme when values from Table IV of $\Delta G_4 = -9.4$ and ΔG_8

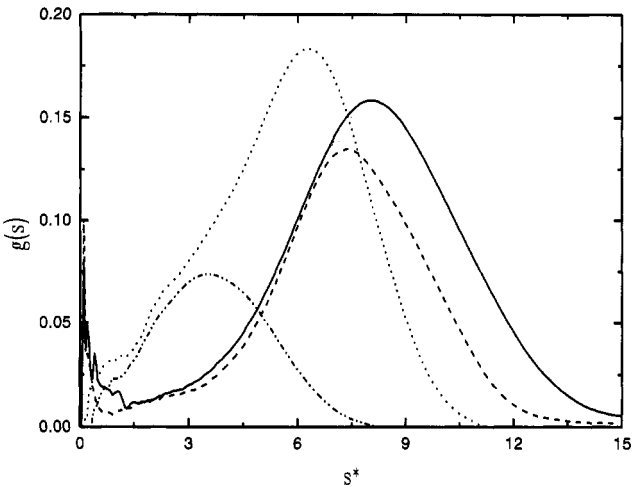

FIGURE 3: Concentration dependence of the sedimentation coefficient distribution function for wild-type repressor at 50 mM KCl. Curves for initial loading concentrations of 126 (—), 58 (– –), 19 (···), and 6.5 μM (– · –) are shown for data acquired at 20 °C and 60K rpm. The channels loaded at 126 and 58 μM were scanned at 296 nm; the channels loaded at 19 and 6.5 μM were scanned at 280 nm. The shift toward lower s^* with decreasing concentration is indicative of mass action self-association. The low s^* trailing edge corresponds to the repressor dimer.

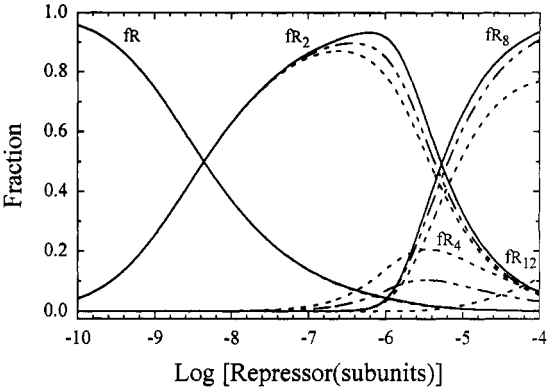

FIGURE 4: Distribution of the different repressor polymeric species versus log concentration of total subunits, from analysis of the sedimentation equilibrium data for the wild-type repressor according to dimer–octamer (solid curves), dimer–tetramer–octamer (broken curves), and dimer–tetramer–octamer–dodecamer (dashed curves) assembly schemes. The curves represent the fractions of total subunits accounted for as monomer, dimer, tetramer, octamer, and dodecamer, as marked. Data were analyzed with σ fixed to reflect the actual repressor dimer molecular weight of 52 400. An equilibrium constant for monomer to dimer assembly of 2.3×10^8 M^{-1} (Koblan & Ackers, 1991) was used. The standard state is 1 M.

= –26.7 kcal/mol are used. The poor fit is indicated by a factor of 2 increase in the variance of the fit and systematic residuals. However, as reflected in the parameter estimates in Table IV, for ΔG_4 less than –7.0 to –7.5 kcal/mol, ΔG_4 and ΔG_8 are highly correlated in fitting the centrifuge data, such that both parameters decrease together with only negligible changes in the variance of the fit. Therefore, considering both the sedimentation equilibrium data and the anisotropy data together, it is likely that $\Delta G_4 \geq -7.5$ kcal/mol and that $\Delta G_8 \approx -23.0$ kcal/mol for I84S at low salt. $\Delta G_4 \geq -7.5$ kcal/mol is in line with estimates for the wild-type repressor and Y88C mutant at low salt and all the proteins at high salt.

Sedimentation Velocity. Sedimentation velocity experiments were conducted for the wild-type repressor at four repressor concentrations (6.5, 19, 58, and 126 μM) which span the dimer to octamer assembly transition. Experiments were conducted at both high- and low-salt conditions. Under high-salt conditions, apparent sedimentation coefficients of 5.4, 7.2, 7.6, and 7.7 S were obtained, respectively. At low salt, the respective apparent sedimentation coefficients are 4.4, 6.4, 8.7, and 9.4 S.

At each concentration, the sedimentation coefficient distribution was calculated (Stafford, 1992). Distributions calculated from the low-salt data are shown in Figure 3. A broad distribution of sedimentation coefficients is obtained at each repressor concentration. The presence of a single peak in the distribution could be indicative that one oligomeric species is dominant. However, the peak s value increases monotonically over this concentration range to a limiting value near 9 S. These observations conform to results from the sedimentation equilibrium analysis, which demonstrate that a self-assembly equilibrium is present at every concentration over this range (see Figure 4). As a result, the sedimentation coefficients do not reflect discrete species. Rather, they reflect an average for all of the species present. Moreover, the apparent distributions are affected by the kinetics of the assembly reaction as demonstrated by a distinct shift to lower s^* in the peak when the analyses were conducted at 30K rpm rather than 60K rpm. This suggests that the kinetics of dissociation of the higher order polymers are extremely slow, with half-lives on the order of tens of minutes. At high salt, $g(s)$ analysis revealed both a peak at 6 S and a shoulder at 9 S. This is indicative of the presence of more than one oligomeric form. The similarity between the sedimentation coefficients from the $g(s)$ plots at high and low salt suggests that the same oligomeric species are present under these two conditions.

DISCUSSION

Dimer–Octamer Assembly. The goal of our studies is to dissect the energetics of cooperativity in λ *c*I repressor binding to the λ operators O_R and O_L into the contributions from different macromolecular processes. The strategy is to compare the energetics of higher order assembly of free solution repressor dimers to the assembly energetics of dimers bound both to single-operator and to multiple-operator DNA. Here, we have reported on the assembly of free repressor dimers in the absence of operator DNA binding, comparing wild-type repressor (both Trp containing and 5-OHTrp containing) and two mutant repressors, I84S and Y88C.

Figure 4 presents the distribution of polymeric species for the wild-type repressor at high salt, according to the three assembly schemes (Table II) that are consistent with the sedimentation equilibrium data (Figure 1). It is clear that between 10^{-6} and 10^{-4} M in total repressor subunits, dimer and octamer are the predominant species. While tetramers do appear to form, they do so only as minor intermediates in the pathway of assembly of dimers to octamers. Dodecamers or other high molecular weight species must predominate in the millimolar concentration range, but are negligible below 10^{-4} M. The transition from octamer to higher molecular weight species appears to reflect the eventual solubility limit of the repressor. Therefore, it was impossible to completely characterize this transition. However, estimation of tetramer and octamer concentrations below 10^{-6} M total repressor, i.e., the concentration range over which repressor interacts with O_R and O_L, is not significantly affected by the assembly beyond octamer.

Separate analyses of the self-association of wild-type repressor at low salt, and of the self-association of the other repressors at both high and low salt, fully support these conclusions. On the basis of the values in Table IV, the best parameter estimates for wild-type repressor are $\Delta G_4 = -7.0$

± 0.3 and $\Delta G_8 = -23.1 \pm 0.4$ kcal/mol. In free energy terms, tetramers are not a predominant species because the assembly free energy change *per dimer unit* (two) to form tetramers (–3.5 kcal/mol) is significantly less then the free energy change *per dimer unit* (four) to form octamers (–5.8 kcal/mol). Thus, the assembly of dimers to octamers is a concerted process.

The steady-state fluorescence anisotropy data for the I84S repressor are particularly useful to define ΔG_4. The maximum steady-state anisotropy of both wild-type and I84S repressors at 50 mM KCl is significantly smaller than that observed for *N*-acetyltryptophanamide in glycerol (0.059 ± 0.001 versus 0.161). In addition to the global motion of a protein, both segmental motion and energy transfer can further reduce the steady-state fluorescence anisotropy of a tryptophan residue. Our previous study of the anisotropy decay of the repressor suggests considerable segmental motion of the tryptophan-containing C-terminal domain (Ross et al., 1992). In addition, with excitation at 270 nm, there is the possibility of both tyrosine-to-tryptophan and tryptophan-to-tryptophan excitation resonance energy transfer. The anisotropy increase observed for dimerization of the repressor could be explained by a change in the mean fluorescence lifetime or by changes in segmental and global motions. Since the fluorescence intensity of the repressor remains strictly proportional to protein monomer concentration, there is no significant change in the fluorescence lifetime associated with dimerization. In addition, we find that the fluorescence intensity decays for 1 μM wild-type, I84S, and Y88C repressors are identical, despite significant differences in monomer, dimer, and higher order oligomer distributions. Consequently, the anisotropy change is dominated by changes in protein motions, and can be treated as strictly a molar quantity. Assembly to larger oligomers results in no further increase in the steady-state anisotropy. This suggests that there is no further change in segmental motions (or energy transfer) accompanying higher order assembly, and supports the analysis of these data using eq 3.

The basic observation, that repressor dimers assemble to form octamers as the limiting species over the subunit concentration range 10^{-6}–10^{-4} M, is entirely consistent with observations reported over 15 years ago by Brack and Pirrotta (1975). They described an M_r 50 000 species undergoing mass action assembly to forms of at least M_r 160 000–180 000 over this same concentration range. These earlier data were interpreted incorrectly as indicating tetramer as the predominant species. This interpretation was based on the sedimentation coefficient of 6.2 S obtained using sucrose gradient centrifugation at 10^{-5} M repressor (Pirotta et al., 1970). We agree that 6.2 S is a reasonable sedimentation coefficient for tetrameric repressor. In fact, the sedimentation coefficient that we observe as corresponding to the peak in the distribution at 19 μM repressor (Figure 3) is 6.4 S. However, according to the sedimentation equilibrium results, at this concentration the repressor is composed primarily of octamer and of dimer, with only small amounts of tetramer.

Another study of the higher order assembly of λ repressor by Banik et al. (1993) was published after our report was originally submitted. This used steady-state fluorescence anisotropy of dansyl-labeled repressor as the experimental observable. In the interpretation of their data, the authors chose to accept the dimer–tetramer stoichiometry proposed by Pirotta (Pirotta et al., 1970). Unfortunately, the relatively short fluorescence lifetime of the dansyl probe compared to the global rotational correlation time of any assembly larger than dimer, as well as the substantial noise in the data, combined to preclude accurate assessment of the assembly stoichiometry based on the shape of the anisotropy change. Interpretation of the anisotropy change in terms of a dimer–tetramer stoichiometry was supported by nonequilibrium methods (including small-zone gel permeation chromatography and Ferguson analysis of polyacrylamide gel electrophoresis) to estimate the molecular weight of the limiting oligomeric form. In the column experiments, the repressor sample was loaded at concentrations at which, as we show here, octamer predominates. The peak concentrations eluted were much lower, in the range for which, as we also show here, both dimer and octamer, but little tetramer, are present. Nevertheless, the elution volume was interpreted as indicating tetramer to be the limiting oligomeric form at the peak concentration eluted. Unfortunately, as is generally well-known, there is no simple relationship between the elution volume for a self-assembling system in a small-zone experiment and either the concentration of protein loaded or the peak concentration eluted (Ackers, 1970). In addition, the authors also note that the anisotropy change appears to take place over about a 10-fold concentration range. Clearly, this transition is too steep to account for dimer–tetramer assembly. However, it is consistent with dimer–octamer assembly. It is impossible to assess the effect of fitting noisy data to the wrong assembly model. Self-assembly is an asymmetric transition, and we note that in several cases the data of Banik et al. (1993) do not bracket the midpoint of the transition. Therefore, it is questionable whether there is any utility to the thermodynamic parameters that they have reported.

Shape of the Octamer. Interpretation of the sedimentation coefficient distribution data in terms of sedimentation coefficients of individual oligomeric repressor species is difficult. The trailing edge at the lowest concentrations is 2–3 S and corresponds to repressor dimer. Continuous dilution of the repressor on the trailing edge will necessarily skew the distribution toward smaller *s* values, as compared to the distribution for the equilibrium mixture of oligomeric forms present at the loading concentration at the start of the experiment. The sedimentation coefficient distributions determined under high-salt conditions indicated greater effects due to kinetic artifacts of this sort than do the data in Figure 3. The data in Figure 3 are likely to be more representative of the initial distribution then the data at high salt. The limiting value of the $g(s)$ peak at high repressor concentration suggests a sedimentation coefficient of about 8–9 S for the octamer. On the basis of a sedimentation coefficient of 8–9 S, the shape of the octamer can be modeled as a prolate ellipsoid (Waxman et al., 1993). This analysis predicts a major axis of about 300 Å. This is the length of about 90 bp of DNA helix. This length of DNA would accommodate four 17 bp operator sites, arranged as in O_R and O_L, with 6–7 bp spacing between operators.

Roles for Tetramer and for Octamer in Cooperativity. Figure 5 shows the concentrations of the various oligomeric forms of the repressor over the physiological range of repressor concentrations in a λ lysogen. It is instructive to compare dimer, tetramer, and octamer concentrations to those which would be necessary to half-saturate the operator sites, assuming that the higher order forms, tetramer and octamer, are capable of simultaneously binding to two or to three operator sites, respectively, and with the same intrinsic binding free energy changes as for dimer binding. Consider tetramer, for example. At 200 mM KCl, the free energy changes for intrinsic binding of repressor dimer to O_R1, O_R2, and O_R3 are $\Delta G_1 = -12.8$, $\Delta G_2 = -11.0$, and $\Delta G_3 = -9.9$ kcal/mol (Senear & Batey, 1991). Figure 5 indicates that at the dimer concentration

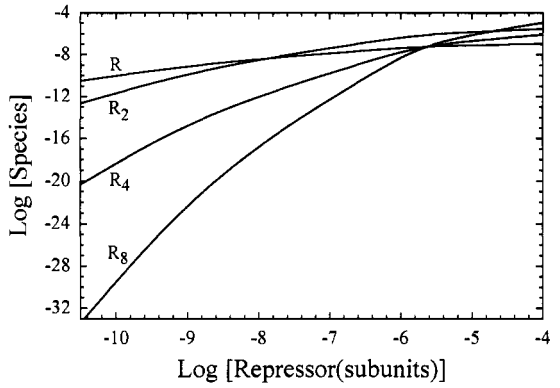

FIGURE 5: Concentrations of the repressor species monomer, dimer, tetramer, and octamer over the range of total repressor concentrations where repressor binds cooperatively to O_R. The curves reflect the analysis of the sedimentation equilibrium data (Figure 1) for the wild-type repressor in 200 mM KCl as described in the legend to Figure 3. The standard state is 1 M.

sufficient to half-saturate O_R1 (2.8×10^{-10} M), the tetramer concentration approaches 10^{-14} M. This estimate could be inaccurate by as much 1–2 orders of magnitude, given the experimental uncertainty in the free energy changes determined here for dimer–tetramer and for dimer–octamer assembly. Nevertheless, even 10^{-16} M is still far in excess of the concentration needed for tetramer to simultaneously half-saturate O_R1 and O_R2 (2×10^{-18} M) if tetramer were to bind with the sum of the free energy changes for dimer binding independently to O_R1 and to O_R2.

A similar result is obtained if the concentration of octamer is compared to that required to simultaneously half-saturate all three operator sites, again assuming a binding free energy change equal to the sum of the free energy changes for dimer binding separately to O_R1, O_R2, and O_R3. At a dimer concentration of 2.8×10^{-10} M, sufficient to half-saturate O_R1, the octamer concentration exceeds the equilibrium dissociation constant for simultaneous interaction with all three operators [defined by $\exp[-(\Delta G_1 + \Delta G_2 + \Delta G_3)/RT]$] by greater than 10^4-fold. Because the assembly of dimer to octamer is a concerted process, the ratio of octamer concentration to this dissociation constant is always greater than the ratio of the tetramer concentration to the dissociation constant, defined by $\exp[-(\Delta G_1 + \Delta G_2)/RT]$. Therefore, octamer might be expected to compete effectively with tetramer for binding to O_R (and O_L), even with one of its four potential operator binding sites left unliganded. Our recent studies of the 5-OHTrp-containing wild-type repressor in the presence of a stoichiometric excess of single-operator, O_R1 oligonucleotide (Laue et al., 1993) demonstrated binding of multiple (i.e., a minimum of about 3) oligonucleotides to the octamer, indicating that the DNA binding sites are not occluded.

Johnson et al. (1979) first proposed the specific features of cooperativity that have formed the basis for current models of the interaction of the λ repressor with the λ operators. These features were based on semiquantitative estimates of the apparent binding affinities of the repressor for the operator sites of O_R and several reduced-valency mutants of O_R. According to the current view (Ptashne, 1992), cooperativity is strictly pairwise and involves only adjacent operator sites. Cooperative interaction between repressor bound to O_R2 and O_R3 is possible only when repressor is not bound to O_R1. These features were critically evaluated by Ackers and coworkers (Senear & Ackers, 1990). Their analysis was based on complete individual-site binding isotherms for interaction of repressor with O_R and reduced-valency mutants of O_R. It confirmed that cooperativity involves only adjacent operator sites. It also demonstrated that cooperativity between O_R2 and O_R3 is possible with repressor bound to O_R1, and it raised the question whether cooperativity with all three operator sites liganded represents a single three-way interaction, as described by the unique free energy change, ΔG_{123}, rather than a statistical average of the two pairwise cooperative free energy changes, ΔG_{12} and ΔG_{23}. Unfortunately, these two models are numerically equivalent for O_R under most experimental conditions studied. Consequently, an unequivocal determination of the molecular basis for cooperativity when all three operator sites are liganded is not possible based on thermodynamic data from binding experiments. However, on the basis of the results reported here, octamer is a species that might be capable of making a three-way interaction by binding simultaneously to all three operator sites.

Strategy To Resolve Contributions to the Cooperative Free Energy Changes. It is clear from the relative concentrations of dimer, tetramer, and octamer (Figure 5) that octamer must bind to three sites simultaneously with a free energy change that is *less* than the sum of the intrinsic free energy changes for dimer binding separately to the three sites. If this were not the case, dimer and tetramer could not compete with octamer for binding, and O_R would be a simple two-state switch, unliganded or fully liganded. Similarly, tetramer must bind simultaneously to two operators with a free energy change that is less than the sum of the intrinsic free energy changes for dimer binding separately to two sites. Otherwise, singly liganded operator states could not exist. We conclude that one or more other mechanisms (structural rearrangements of the repressor assembly, structural rearrangements of the DNA, linkage between assembly and operator binding, or allostery) make an unfavorable contribution to cooperativity and prevent this situation.

Figure 6 presents a scheme for binding of the different repressor oligomers to single-operator DNA. Linkage between repressor assembly and DNA binding exists if the free energy changes for binding of the first operator oligonucleotide to dimer ($^2\Delta G_1$), to tetramer ($^4\Delta G_1$), and to octamer ($^8\Delta G_1$) differ from one another. Allostery that is mediated by the repressor exists if the free energy changes for the binding of successive operator oligonucleotides to the tetramer ($^4\Delta G_1$ versus $^4\Delta G_2$) or to the octamer ($^8\Delta G_1$, $^8\Delta G_2$, $^8\Delta G_3$, $^8\Delta G_4$) differ from one another. Both linkage and allostery produce free energy changes for dimer–tetramer and for dimer–octamer assembly that are different when the repressor is bound to the operator oligonucleotide than when it is free in solution. To determine if either linkage or allostery contributes to cooperativity, self-association studies of repressor bound to single-operator oligonucleotide can be conducted. Possible results are that operator binding either favors or disfavors assembly of dimers to higher order forms, that operator binding preferentially either stabilizes or destabilizes either tetramer or octamer, or that operator binding has no effect. Experiments are currently in progress to answer this question.

Simultaneous interaction of repressor oligomers with multiple operator sites is likely to require structural rearrangement of either protein, DNA, or both, and, therefore, it will contribute unfavorably to cooperativity. A contribution from this mechanism can be identified by studying the assembly of repressor when bound to multiple-operator DNA. In these experiments, a spectral signal from the DNA can be used to monitor the distribution of DNA-bound species. For example, triple-operator DNA might preferentially associate either with octamer or with tetramer plus dimer. Using resonance energy

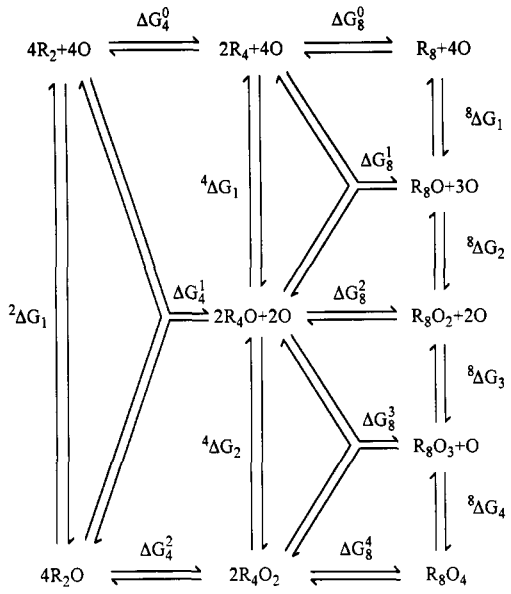

FIGURE 6: Linkage scheme showing the effect of single-site operator binding on the self-assembly of repressor dimers. O denotes single-operator oligonucleotide. R_2, R_4, and R_8 denote repressor dimer, tetramer, and octamer, respectively. The free energy changes for dimer–tetramer and for dimer–octamer association of unliganded repressor are denoted by ΔG_4^0 and ΔG_8^0, respectively. Corresponding free energy changes for operator-bound repressor are denoted by ΔG_4^i and ΔG_8^i, where the value of the superscript denotes the stoichiometry of bound operator oligonucleotide in the product repressor oligomer. The stepwise free energy changes for successive operator binding to dimers, tetramers, and octamers are denoted by $^2\Delta G_i$, $^4\Delta G_i$, and $^8\Delta G_i$, respectively.

transfer between 5-OHTrp incorporated in the repressor as donor and fluorescent labels bound to oligonucleotides as acceptors, the orientation of the various oligomeric repressor species bound to multiple-operator DNA can be determined. In these ways, we expect to ascertain the exact role of the different repressor oligomeric species in regulation of O_R and O_L.

ACKNOWLEDGMENT

We acknowledge scientific discussions with Dr. Carol Hasselbacher, Dr. William Laws, and Dr. Reza Green. We are particularly grateful for the extremely useful comments of Dr. Laws. We appreciate the technical assistance of Theresa M. Ridgeway, Yao Te Huang, and Laura Perini. We thank Dr. Robert Sauer for his kind gift of the mutant repressor expression plasmids.

REFERENCES

Ackers, G. K. (1970) *Adv. Protein Chem. 24,* 343–446.
Amnan, E., Brosius, J., & Ptashne, M. (1983) *Gene 25,* 167.
Badea, M. G., & Brand, L. (1979) *Methods Enzymol. 61,* 378–425.
Banik, U., Mandal, N. C., Bhattacharyya, B., & Roy, S. (1993) *J. Biol. Chem. 268,* 3938–3943.
Bellomy, G. R., Mossing, M. C., & Record, M. T. (1988) *Biochemistry 27,* 3900–3906.
Brack, C., & Pirrotta, V. (1975) *J. Mol. Biol. 96,* 139–152.
Brenowitz, M., Senear, D. F., Shea, M. A., & Ackers, G. K. (1986) *Methods Enzymol. 130,* 132–181.
Brenowitz, M., Pickar, A., & Jamison, E. (1991) *Biochemistry 30,* 5986–5998.
Cohn, E. J., & Edsall, J. T. (1943) *Proteins, Amino Acids and Peptides as Ions and Dipolar Ions,* Reinhold, New York.
Gralla, J. D. (1989) *Cell 57,* 193–195.
Hecht, M. H., Nelson, H. C. M., & Sauer, R. T. (1983) *Proc. Natl. Acad. Sci. U.S.A. 80,* 2676–2680.
Johnson, A. D., Meyer, B. J., & Ptashne, M. (1979) *Proc. Natl. Acad. Sci. U.S.A. 76,* 5061–5065.
Johnson, A. D., Poteete, A. R., Lauer, G., Sauer, R. T., Ackers, G. K., & Ptashne, M. (1981) *Nature 294,* 217–223.
Johnson, M. L., & Frasier, S. G. (1985) *Methods Enzymol. 117,* 301–342.
Johnson, M. L., Correia, J. C., Yphantis, D. A., & Halverson, H. R. (1981) *Biophys. J. 36,* 575–588.
Koblan, K. S., & Ackers, G. K. (1991) *Biochemistry 30,* 7817–7821.
Laue, T. M. (1981) Ph.D. Dissertation, University of Connecticut, Storres, CT.
Laue, T. M., Shah, B. D., Ridgeway, T. M., & Pelletier, S. M. (1992) in *Analytical Ultracentrifugation in Biochemistry and Polymer Science* (Harding, S., Rowe, A., & Horton, J. C., Eds.) pp 90–125, Royal Society of Chemistry, London.
Laue, T. M., Senear, D. F., Eaton, S., & Ross, J. B. A. (1993) *Biochemistry 32,* 2469–2472.
Mossing, M. C., & Record, M. T. (1986) *Science 233,* 889–892.
Pirotta, V., Chadwick, P., & Ptashne, M. (1970) *Nature 227,* 41–44.
Ptashne, M. (1992) *A Genetic Switch,* 2nd ed., Cell Press & Blackwell Scientific Publications, Cambridge, MA.
Ross, J. B. A., Senear, D. F., Waxman, E., Kombo, B. B., Rusinova, E., Huang, Y. T., Laws, W. R., & Hasselbacher, C. A. (1992) *Proc. Natl. Acad. Sci. U.S.A. 89,* 12023–12027.
Sauer, R. T., Hehir, K., Stearman, R. S., Weiss, M. A., Jeitler-Nilsson, A., Suchanek, E. G., & Pabo, C. O. (1986) *Biochemistry 25,* 5992–5998.
Senear, D. F., & Ackers, G. K. (1990) *Biochemistry 29,* 6568–6577.
Senear, D. F., & Batey, R. (1991) *Biochemistry 30,* 6677–6688.
Shea, M. A., & Ackers, G. K. (1985) *J. Mol. Biol. 181,* 211–230.
Stafford, W., III (1992) *Anal. Biochem. 203,* 295–301.
Waxman, E., Laws, W. R., Laue, T. M., Nemerson, Y., & Ross, J. B. A. (1993) *Biochemistry 32,* 3005–3012.
Wetlaufer, D. B. (1962) *Adv. Protein Chem. 17,* 303–390.
Yphantis, D. A. (1960) *Ann. N.Y. Acad. Sci. 88,* 586–601.
Yphantis, D. A. (1964) *Biochemistry 3,* 297–317.
Yphantis, D. A., & Waugh, D. F. (1956) *J. Phys. Chem. 60,* 623–629.